arXiv:1404.0482v1 [cond-mat.supr-con] 2 Apr 2014

Controllable Rashba spin-orbit interaction in artificially engineered superlattices involving the heavy-fermion superconductor $CeCoIn_5$

M. Shimozawa[1], S. K. Goh[1,2], R. Endo[1], R. Kobayashi[1], T. Watashige[1], Y. Mizukami[1], H. Ikeda[1], H. Shishido[3], Y. Yanase[4], T. Terashima[5], T. Shibauchi[1], and Y. Matsuda[1]
[1]*Department of Physics, Kyoto University, Kyoto 606-8502, Japan*
[2]*Cavendish Laboratory, University of Cambridge, JJ Thomson Avenue, Cambridge CB3 0HE, United Kingdom*
[3]*Department of Physics and Electronics, Osaka Prefecture University, Osaka 599-8531, Japan*
[4]*Department of Physics, Niigata University, Niigata 950-2181, Japan and*
[5]*Research Center for Low Temperature and Materials Science, Kyoto University, Kyoto 606-8501, Japan*
(Dated: April 3, 2014)

By using a molecular beam epitaxy technique, we fabricate a new type of superconducting superlattices with controlled atomic layer thicknesses of alternating blocks between heavy fermion superconductor $CeCoIn_5$, which exhibits a strong Pauli pair-breaking effect, and nonmagnetic metal $YbCoIn_5$. The introduction of the thickness modulation of $YbCoIn_5$ block layers breaks the inversion symmetry centered at the superconducting block of $CeCoIn_5$. This configuration leads to dramatic changes in the temperature and angular dependence of the upper critical field, which can be understood by considering the effect of the Rashba spin-orbit interaction arising from the inversion symmetry breaking and the associated weakening of the Pauli pair-breaking effect. Since the degree of thickness modulation is a design feature of this type of superlattices, the Rashba interaction and the nature of pair-breaking are largely tunable in these modulated superlattices with strong spin-orbit coupling.

PACS numbers: 71.27.+a, 74.70.Tx, 74.78.Fk, 81.15.Hi

Among the existing condensed matter systems, the metallic state with the strongest electron correlation effects is achieved in heavy fermion materials with $4f$ or $5f$ electrons. In these systems, a very narrow conduction band is formed at low temperatures through the Kondo effect. In particular, in Ce($4f$)-based compounds, strong electron correlations within the narrow band strikingly enhance the quasiparticle effective mass. As a result of notable many-body effects, a plethora of fascinating physical phenomena including unconventional superconductivity with non-s-wave pairing symmetry appears [1]. The unconventional pairing symmetry and the associated exotic superconducting properties have mystified researchers over the past quarter century.

Recently, it has been suggested that the inversion symmetry breaking (ISB) together with strong spin-orbit interaction can dramatically affect the superconductivity, giving rise to a number of novel phenomena such as anomalous magneto-electric effects [2] and topological superconducting states [3–5]. It has also been pointed out that such phenomena are more pronounced in strongly correlated electron systems [6]. The inversion symmetry imposes important constraints on the pairing states: In the presence of inversion symmetry, Cooper pairs are classified into a spin-singlet or triplet state, whereas in the absence of inversion symmetry, an asymmetric potential gradient ∇V yields a spin-orbit interaction that breaks parity, and the admixture of spin singlet and triplet states is possible [7, 8]. For instance, asymmetry of the potential in the direction perpendicular to the two-dimensional (2D) plane $\nabla V \parallel [001]$ induces Rashba spin-orbit interaction $\alpha_R \boldsymbol{g}(\boldsymbol{k}) \cdot \boldsymbol{\sigma} \propto (\boldsymbol{k} \times \nabla V) \cdot \boldsymbol{\sigma}$, where $\boldsymbol{g}(\boldsymbol{k}) = (-k_y, k_x, 0)/k_F$, k_F is the Fermi wave number, and $\boldsymbol{\sigma}$ is the Pauli matrix. Rashba interaction splits the Fermi surface into two sheets with different spin structures: the energy splitting is given by α_R, and the spin direction is tilted into the plane, rotating clockwise on one sheet and anticlockwise on the other. When the Rashba splitting exceeds the superconducting gap energy ($\alpha_R > \Delta$), the superconducting properties are dramatically modified. Therefore, in Ce-based superconductors, where the spin-orbit interaction is generally significant, the introduction of ISB makes the systems a fertile ground for observing exotic properties. Although there are bulk heavy fermion superconductors with ISB such as $CePt_3Si$ [9] and $CeRhSi_3$ [10], their superconductivity often coexists with magnetic order and the degree of the ISB is hard to be controlled. Thus the systematic influence of ISB on unconventional superconductivity remains an open question.

$CeCoIn_5$ is a heavy fermion superconductor [11] which hosts a wide range of fascinating superconducting properties including extremely strong Pauli pair-breaking effect [12–16] and an associated possible Fulde-Ferrell-Larkin-Ovchinnikov (FFLO) state with a novel pairing state ($\boldsymbol{k}\uparrow$, $-\boldsymbol{k}+\boldsymbol{q}\downarrow$) [17–21]. Although the crystal structure of bulk $CeCoIn_5$ possesses the inversion symmetry, band structure calculations suggest that even a small degree of ISB can induce a large Rashba splitting of the Fermi surface [22]. Recently, a state-of-the-art molecular beam epitaxy technique has been developed to fabricate the c axis oriented artificial superlattices with alternating

layers of $CeCoIn_5$ and nonmagnetic, nonsuperconducting metal $YbCoIn_5$ with controlled atomic layer thicknesses [23–26]. In these superlattices, RKKY interaction between the Ce atoms in neighboring $CeCoIn_5$ block layers is substantially reduced [27]. Moreover, the superconducting proximity effect between $CeCoIn_5$- and $YbCoIn_5$-layers is negligibly small due to the large Fermi velocity mismatch [28]. In fact, it has been shown that in the superlattices with 4–6 unit cell thick $CeCoIn_5$ layers, whose thickness is comparable to the perpendicular coherence length $\xi_\perp \sim$3–4 nm, 2D heavy fermion superconductivity is realized [24]. In these superlattices, the importance of the *local* ISB at the interface between $CeCoIn_5$ and $YbCoIn_5$ has been emphasized experimentally through the peculiar angular variation of upper critical field H_{c2}, which can be interpreted as a strong suppression of the Pauli pair-breaking effect [25]. Theoretical studies also suggest that when the interlayer hopping integral is comparable to or smaller than the Rashba splitting ($t_c \lesssim \alpha_R$), the local ISB plays an important role in determining the nature of the superconducting state [29]. This appears to be the case for the $CeCoIn_5/YbCoIn_5$ superlattices.

To advance the understanding of the effect of the ISB on the superconducting ground state, we designed and fabricated a new type of superlattices, i.e. *modulated* superlattices in which the thickness of $CeCoIn_5$ is kept to n for the entire superlattice, while the thickness of $YbCoIn_5$ alternates between m and m' from one block layer to the next, forming a (n:m:n:m') c axis oriented superlattice structure. We demonstrate that, through the introduction of the thickness modulation of $YbCoIn_5$ layers, the Rashba effect in each superconducting $CeCoIn_5$ block layer is largely tunable, leading to profound changes in the nature of superconductivity. This "block tuning" of Rashba interaction appears to pave the way for obtaining novel superconducting states.

We study superlattices both without and with thickness modulation of $YbCoIn_5$ layers, $m = m'$ (Fig. 1(a)) and $m \neq m'$ (Fig. 1(b)), respectively (for the fabrication method, see Sec. S1 in [30]). We denote the former as S-type and the latter as S*-type superlattices. In both superlattices, the asymmetric potential gradient associated with the local ISB, $-\nabla V_{\rm local}$, gives rise to the Rashba splitting. This splitting is the largest at the top and bottom $CeCoIn_5$ layers and vanishes at the middle layer, as shown by the green (small) arrows in Figs. 1(a) and (b). The critical difference between the S- and S*-type superlattices is that, as illustrated in Figs. 1(a) and (b), for the S-type superlattices, the middle Ce plane in a given $CeCoIn_5$ block layer is a mirror plane, whereas for the S*-type it is not. In the S*-type superlattices, therefore, the additional ISB along the c-axis can be introduced to the superconducting $CeCoIn_5$ block layers. The asymmetric potential gradient associated with the $YbCoIn_5$ thickness modulation, $-\nabla V_{\rm block}$, point to the opposite direction in the neighboring $CeCoIn_5$-block layers as shown by the orange (large) arrows in Fig. 1(b). (We note that even in the S*-type one can find mirror planes in $YbCoIn_5$ layers but here we focus mainly on the ISB in the superconducting planes.) We expect that the degree of this "*block layer* ISB" (BLISB) can be enhanced with increasing $|m - m'|$, which represents the degree of thickness modulation.

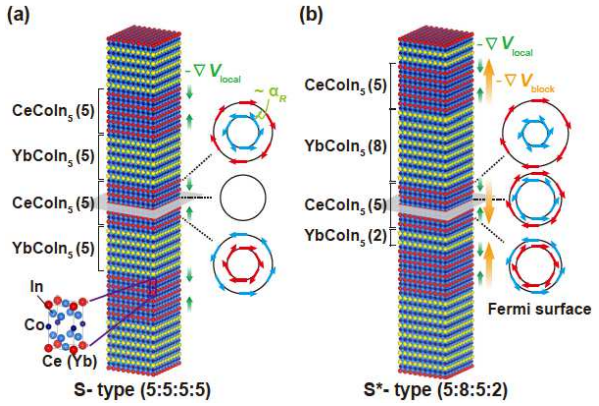

FIG. 1. (color online). Schematic representations of the $CeCoIn_5(n)/YbCoIn_5(m)/CeCoIn_5(n)/YbCoIn_5(m')$ artificial superlattices. (a) S-type ($m = m'$): Superlattice with alternating layers of 5-UCT $CeCoIn_5$ and 5-UCT $YbCoIn_5$, (n:m:n:m') = (5:5:5:5). The middle $CeCoIn_5$ layer in a given $CeCoIn_5$ block layer indicated by the gray plane is a mirror plane. The green (small) arrows represent the asymmetric potential gradient associated with the local ISB, $-\nabla V_{\rm local}$. The Rashba splitting occurs at the interface between the $CeCoIn_5$ and $YbCoIn_5$ due to the local ISB. The spin direction is rotated in the ab plane and is opposite between the top and bottom $CeCoIn_5$ layers. (b) S*-type ($m \neq m'$): 5-UCT $CeCoIn_5$ block layers are sandwiched by 8- and 2-UCT $YbCoIn_5$ layers, (n:m:n:m') = (5:8:5:2). The middle $CeCoIn_5$ layer (gray plane) is not a mirror plane. The orange (large) arrows represent the asymmetric potential gradient associated with the $YbCoIn_5$ layer thickness modulation $-\nabla V_{\rm block}$.

Here we stress that one of the most remarkable effects of the ISB on the superconductivity appears in the magnetic response: the Zeeman term in magnetic field in the presence of Rashba interaction is given by $\pm \boldsymbol{g}(\boldsymbol{k}) \cdot \mu_0 \boldsymbol{H}$, which leads to a strong suppression of the Pauli pair-breaking effect, in particular for $\boldsymbol{H} \parallel c$ where $\boldsymbol{g}(\boldsymbol{k})$ is always perpendicular to $\boldsymbol{H}$ [7, 8]. It is therefore of tremendous interest to experimentally introduce the ISB in $CeCoIn_5$ with strong Pauli-limited superconductivity, for this will allow the study of its interplay with the strong Pauli pair-breaking effect and its influence on the unconventional superconductivity of an archetypal heavy fermion superconductor.

To examine how the BLISB affects the superconductivity of the 2D $CeCoIn_5$ block layers, we fabricated the S- and S*-type superlattices, which consist of 5 unit-cell thick (UCT) $CeCoIn_5$ ($n = 5$) sandwiched by m- and m'-UCT $YbCoIn_5$, whose total number is fixed as $m + m' = 10$ (For the structural characterization, see

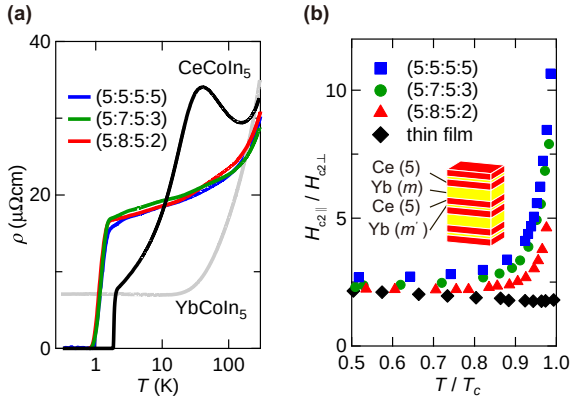

FIG. 2. (color online). (a) Temperature dependence of the resistivity in each superlattice, along with that of 120-nm-thick $CeCoIn_5$ and $YbCoIn_5$ epitaxial thin films. T_c, defined as the temperature where the resistance is 50% of the normal state resistance, is 1.16, 1.18 and 1.13 K for $(n{:}m{:}n{:}m') = (5{:}5{:}5{:}5)$, $(5{:}7{:}5{:}3)$ and $(5{:}8{:}5{:}2)$, respectively. (b) Temperature dependence of the anisotropy of upper critical field H_{c2}, $H_{c2\parallel}/H_{c2\perp}$ for the superlattices and $CeCoIn_5$ thin film.

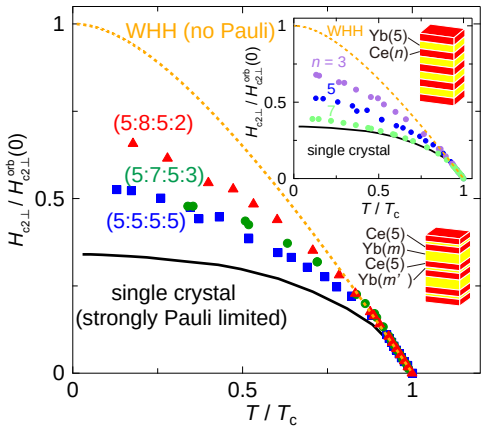

FIG. 3. (color online). Normalized upper critical field $H_{c2\perp}/H_{c2\perp}^{\rm orb}(0)$ as a function of T/T_c for S*-type superlattices with $(n{:}m{:}n{:}m') = (5{:}7{:}5{:}3)$ and $(5{:}8{:}5{:}2)$ compared with that for S-type $(5{:}5{:}5{:}5)$. We also plot $H_{c2\perp}/H_{c2\perp}^{\rm orb}(0)$ for $CeCoIn_5$ single crystal with strong Pauli pair-breaking effect and the WHH curve without the Pauli pair-breaking effect. Inset: The same plot for S-type $CeCoIn_5(n)/YbCoIn_5(5)$ superlattices.

Sec. S2 in Ref. [30]). As shown in Fig. 2(a), the resistivity of the S-type superlattice with $(n{:}m{:}n{:}m') = (5{:}5{:}5{:}5)$ and S*-type superlattices with $(n{:}m{:}n{:}m') = (5{:}7{:}5{:}3)$ and $(5{:}8{:}5{:}2)$ exhibits very similar behavior. Figure 2(b) shows the anisotropy of upper critical fields $H_{c2\parallel}/H_{c2\perp}$. In sharp contrast to the $CeCoIn_5$ thin film with thickness of 120 nm, $H_{c2\parallel}/H_{c2\perp}$ of superlattices exhibits a diverging behavior while approaching T_c, indicating a 2D superconducting behavior.

Figure 3 displays the temperature dependence of $H_{c2\perp}$ normalized by the orbital limited upper critical field without the Pauli pair-breaking effect at $T = 0$ K, $H_{c2\perp}^{\rm orb}(0)$, for $(n{:}m{:}n{:}m') = (5{:}5{:}5{:}5)$, $(5{:}7{:}5{:}3)$ and $(5{:}8{:}5{:}2)$. Here $H_{c2\perp}^{\rm orb}(0)$ is calculated by the Werthamer-Helfand-Hohenberg (WHH) formula [31], $H_{c2\perp}^{\rm orb}(0) = -0.69T_c({\rm d}H_{c2\perp}/{\rm d}T)_{T_c}$. We also include the two extreme cases, $H_{c2\perp}/H_{c2\perp}^{\rm orb}(0)$ for the bulk $CeCoIn_5$ [13], in which superconductivity is dominated by Pauli paramagnetism, and WHH curve without the Pauli pair-breaking effect. What is remarkable is that at low temperatures $H_{c2\perp}/H_{c2\perp}^{\rm orb}(0)$ is enhanced with increasing $|m-m'|$. This is in sharp contrast to the case of bulk $Ce_{1-x}Yb_xCoIn_5$ system [32], where the chemical substitution of Ce with Yb does not change the whole temperature dependence of $H_{c2\perp}/H_{c2\perp}^{\rm orb}(0)$. Because the resistivity of these superlattices shows a very similar temperature dependence with similar T_c as displayed in Fig. 2(a), this enhancement cannot be attributed to the difference in the electron scattering rate or impurity concentration. We can also rule out the possibility that the enhancement is related to the difference in the spin-orbit scattering (see Sec. S3 in [30]). The enhancement is rather associated with the reduction in the Maki parameter α_M, which represents the ratio of the orbital-limited upper critical field to the Pauli-limited one. Thus the present results suggest that the BLISB modifies the superconducting properties, leading to the relative suppression of the Pauli pair-breaking effect with respect to the orbital pair-breaking effect.

The suppression of the Pauli pair-breaking effect in the S*-type superlattices can be demonstrated clearly by the angular dependence of H_{c2}. Figure 4(a) shows $H_{c2}(\theta)$ of the (5:8:5:2) superlattice determined by the resistive transitions in magnetic fields, where θ is the angle between $\boldsymbol{H}$ and the a-axis. $H_{c2}(\theta)$ increases monotonically without saturation as $|\theta|$ decreases and a distinct cusp behavior is observed at $\theta = 0°$. In sharp contrast, in (5:7:5:3) and (5:5:5:5) superlattices, the cusp structure is not observed and $H_{c2}(\theta)$ is smooth for all θ (Fig. 4(b)). This remarkable difference of $H_{c2}(\theta)$ between S-type (5:5:5:5) and S*-type (5:8:5:2) superlattices is highly unusual because the $CeCoIn_5$ block layers in each superlattice have the same thickness ($n = 5$), and hence similar angular variation of $H_{c2}(\theta)$ is expected, in particular near T_c where $\xi_\perp(T)$ well exceeds the thickness of $CeCoIn_5$ block layer. In order to be more quantitative, we analyze the data using the model below [25]:

$$\left[\frac{H_{c2}(\theta)\cos\theta}{H_{c2}(0°)}\right]^2 + \beta_T\left|\frac{H_{c2}(\theta)\sin\theta}{H_{c2}(90°)}\right| + \beta_P\left[\frac{H_{c2}(\theta)\sin\theta}{H_{c2}(90°)}\right]^2 = 1, \quad (1)$$

where β_T (≥ 0) and β_P (≥ 0) are fitting parameters with $\beta_T + \beta_P = 1$. In Eq. (1) $(\beta_T, \beta_P) = (1, 0)$ represents the so-called Tinkham model [33] which describes $H_{c2}(\theta)$ in the 2D thin film with thickness smaller than $\xi_\perp$ in the absence of the Pauli pair-breaking effect. In the Tinkham model, cusp appears at $\theta = 0$ as a result of the vortex formation due to the orbital pair-breaking effect in a slightly tilted field, which strongly suppresses

H_{c2}. On the other hand, $(\beta_T, \beta_P) = (0, 1)$ represents the anisotropic model, which describes $H_{c2}(\theta)$ of 2D superconductors when Pauli pair-breaking effect dominates. In this case, cusp does not appear because $H_{c2}(\theta)$ is determined by the anisotropy of g-factor, which changes smoothly with θ. Thus β_T/β_P quantifies the relative importance of orbital and Pauli pair-breaking effects. With this model, an excellent description of $H_{c2}(\theta)$ is achieved (Fig. 4(c)). Figure 4(d) shows β_T/β_P for several superlattices at fixed reduced temperatures. For the S*-type superlattices, when going from (5:7:5:3) to (5:8:5:2), β_T/β_P is strongly enhanced, indicating the suppression of the Pauli pair-breaking effect. This result is consistent with the low-temperature enhancement of $H_{c2\perp}/H^{\rm orb}_{c2\perp}(0)$ with increasing $|m-m'|$ shown in Fig. 3. Thus, both the enhancement of $H_{c2\perp}(T)/H^{\rm orb}_{c2\perp}(T=0)$ in perpendicular field and the angular variation of $H_{c2}(\theta)$ around the parallel field indicate that the ISB in the direction perpendicular to the ab-plane strongly affects the superconductivity through the suppression of Pauli paramagnetism, when $|m-m'|$ is tuned from 4 to 6. This result can be understood if the Rashba splitting begins to exceed the superconducting gap energy when $|m-m'|$ reaches a threshold value between 4 and 6.

It has been pointed out that the "local" ISB at interfaces, which results in the Rashba spin-orbit splitting of the Fermi surface of the $CeCoIn_5$ interface layers neighboring the $YbCoIn_5$ layers (Fig. 1(a)), also has an impact on the superconducting properties in the superlattices [25, 29]. In fact, as shown in the inset of Fig. 3, in S-type superlattices with n-UCT $CeCoIn_5$ sandwiched between 5-UCT $YbCoIn_5$ layers, $H_{c2\perp}/H^{\rm orb}_{c2\perp}(0)$ is strikingly enhanced with decreasing n. Moreover, β_T/β_P increases with decreasing n as shown in Fig. 4(d). These results have been interpreted as the increased importance of the local ISB with decreasing n, as the fraction of noncentrosymmetric interface layers increases. Following a similar reasoning, the thickness modulation of $YbCoIn_5$ layers in the S*-type superlattices can be seen as the introduction of an additional ISB to the $CeCoIn_5$ block layers (see Figs. 1(a) and(b)).

Bulk $CeCoIn_5$ hosts an abundance of fascinating superconducting properties. Indeed, $d_{x^2-y^2}$ superconducting gap symmetry is well established [12, 34–38]. Moreover, a possible presence of FFLO phase [17–21] and unusual coexistence of superconductivity and magnetic order [39, 40] at low temperature and high field have been reported. Our $CeCoIn_5$-based superlattices, in which the degree of the ISB and consequently the Rashba splitting in each Ce-block layer are controllable, thus offer the prospect of achieving even more fascinating pairing states than the bulk $CeCoIn_5$. The availability of these superlattices provides a new playground for exploring exotic superconducting states, such as a helical vortex state [41], pair-density-wave state [42], complex-stripe phases [43] , topological superconducting state [3, 4] and Majorana fermion excitations [44], in strongly correlated electron systems. It should be noted that very recently the formation of Majorana flat band has been proposed in the present S*-type superlattice structure [45].

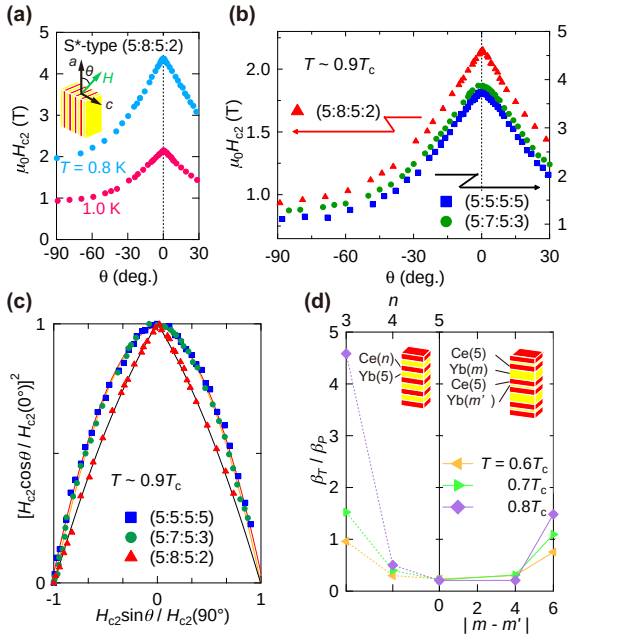

FIG. 4. (color online). Angular dependence of H_{c2} in $CeCoIn_5/YbCoIn_5$ superlattices. (a) $H_{c2}(\theta)$ for the S*-type (5:8:5:2) superlattice. (b) Comparison of $H_{c2}(\theta)$ in (5:8:5:2) (red triangles, left axis), (5:7:5:3) (green circles, right axis) and (5:5:5:5) (blue squares, right axis) superlattices near T_c. (c) H_{c2} of these superlattices near T_c, replotted in an appropriate dimensionless form. The solid lines are the fits to the data using the model described in Eq. (1). (d) β_T/β_P, which quantifies the relative importance of orbital and Pauli pair-breaking effects, is plotted as a function of the thickness modulation of $YbCoIn_5$ layers $|m-m'|$ (right panel). For comparison, β_T/β_P in S-type superlattice $CeCoIn_5(n)/YbCoIn_5(5)$ is plotted as a function of n (left panel).

In summary, we have fabricated a novel type of superconducting superlattices, in which the thickness of $CeCoIn_5$ is kept to n for the entire superlattice, while the thickness of $YbCoIn_5$ alternates between m and m' from one block layer to the next, forming a $(n{:}m{:}n{:}m')$ superlattice structure. Through the measurements of the temperature and angular dependencies of the upper critical field, we find a significant suppression of the Pauli pair-breaking effect in these superlattices when the inversion symmetry breaking is introduced. The magnitude of this suppression increases with the degree of the thickness modulation $|m-m'|$. These results demonstrate that the Rashba spin-orbit interaction in each $CeCoIn_5$ block layer is largely tunable in these modulated superlattices. Our work paves the way for obtaining novel superconducting states through the thickness modulation in the superlattices with strong spin-orbit coupling.

We acknowledge discussions with A. I. Buzdin, S. Fuji-

moto, and M. Sigrist. This work was supported by KAKENHI from the Japan Society for the Promotion of Science (JSPS) and by the "Topological Quantum Phenomena" (Nos. 25103711 and 25103713) Grant-in-Aid for Scientific Research on Innovative Areas from the Ministry of Education, Culture, Sports, Science and Technology (MEXT) of Japan.

[1] C. Pfleiderer, Rev. Mod. Phys. **81,** 1551 (2009).
[2] C. K. Lu and S. Yip, Phys. Rev. B **78**, 132502 (2008).
[3] Y. Tanaka, T. Yokoyama, A. V. Balatsky, and N. Nagaosa, Phys. Rev. B **79**, 060505(R) (2009).
[4] M. Sato and S. Fujimoto, Phys. Rev. B **79**, 094504 (2009).
[5] X. L. Qi and S. C. Zhang, Rev. Mod. Phys. **83**, 1057 (2011).
[6] S. Fujimoto, J. Phys. Soc. Jpn. **76**, 51008 (2007).
[7] L. P. Gor'kov and E. I. Rashba, Phys. Rev. Lett. **87**, 037004 (2001).
[8] P. A. Frigeri, D. F. Agterberg, A. Koga, and M. Sigrist, Phys. Rev. Lett. **92**, 097001 (2004).
[9] E. Bauer *et al.*, Phys. Rev. Lett. **92**, 027003 (2004).
[10] N. Kimura *et al.*, Phys. Rev. Lett. **95**, 247004 (2005).
[11] C. Petrovic *et al.*, J. Phys.: Condens. Matter **13**, L337 (2001).
[12] K. Izawa *et al.*, Phys. Rev. Lett. **87**, 057002 (2001).
[13] T. Tayama *et al.*, Phys. Rev. B **65**, 180504(R) (2002).
[14] A. Bianchi *et al.*, Phys. Rev. Lett. **89**, 137002 (2002).
[15] R. Okazaki, H. Shishido, T. Shibauchi, M. Konczykowski, A. Buzdin, and Y. Matsuda, Phys. Rev. B **76**, 224529 (2007).
[16] A. D. Bianchi *et al.*, Science **11**, 177 (2008).
[17] H. Radovan *et al.*, Nature (London) **425**, 51 (2003).
[18] A. Bianchi, R. Movshovich, C. Capan, P. G. Pagliuso, and J. L. Sarrao, Phys. Rev. Lett. **91**, 187004 (2003).
[19] K Kakuyanagi *et al.* Phys. Rev. Lett. **94**, 047602 (2005).
[20] Y. Matsuda and H. Shimahara, J. Phys. Soc. Jpn **76**, 051005 (2007).
[21] K. Kumagai, H. Shishido, T. Shibauchi, and Y. Matsuda, Phys. Rev. Lett. **106**, 137004 (2011).
[22] H. Ikeda, unpublished.
[23] H. Shishido *et al.*, Science **327**, 980 (2010).
[24] Y. Mizukami *et al.*, Nature Phys. **7**, 849 (2011).
[25] S. K. Goh *et al.*, Phys. Rev. Lett. **109**, 157006 (2012).
[26] M. Shimozawa *et al.* Phys. Rev. B **86**, 144526 (2012).
[27] R. Peters, Y. Tada, and N. Kawakami, Phys. Rev. B **88**, 155134 (2013).
[28] J-H. She and A. V. Balatsky, Phys. Rev. Lett. **109**, 077002 (2012).
[29] D. Maruyama, M. Sigrist, and Y. Yanase, J. Phys. Soc. Jpn. **81**, 034702 (2012).
[30] See Supplemental Material for supplemental data and discussions.
[31] N. R. Werthamer, E. Helfand, and P. C. Hohenberg, Phys. Rev. **147**, 295 (1966).
[32] C. Capan *et al.*, Europhys. Lett. **92**, 47004 (2010).
[33] M. Tinkham, *Introduction to Superconductivity* (McGraw-Hill, New York, 1996), 2nd ed.
[34] W. K. Park, J. L. Sarrao, J. D. Thompson, and L. H. Greene, Phys. Rev. Lett. **100**, 177001 (2008).
[35] C. Stock, C. Broholm, J. Hudis, H. J. Kang, and C. Petrovic, Phys. Rev. Lett. **100**, 087001 (2008).
[36] K. An *et al.*, Phys. Rev. Lett. **104**, 037002 (2010).
[37] M. P. Allan *et al.*, Nature Phys. **9**, 468 (2013).
[38] B. B. Zhou *et al.*, Nature Phys. **9**, 474 (2013).
[39] B.-L. Young, R. R. Urbano, N. J. Curro, J. D. Thompson, J. L. Sarrao, A. B. Vorontsov, and M. J. Graf, Phys. Rev. Lett. **98**, 036402 (2007).
[40] M. Kenzelmann *et al.*, Science **321**, 1652 (2008).
[41] R. P. Kaur, D. F. Agterberg, and M. Sigrist, Phys. Rev. Lett. **94**, 137002 (2005).
[42] T. Yoshida, M. Sigrist, and Y. Yanase, Phys. Rev. B **86**, 134514 (2012).
[43] T. Yoshida, M. Sigrist, and Y. Yanase, J. Phys. Soc. Jpn. **82**, 074714 (2013).
[44] M. Sato and S. Fujimoto, Phys. Rev. Lett. **105**, 217001 (2010).
[45] N. F. Q. Yuan, C. L. M. Wong, and K. T. Law, Physica E, **55**, 30 (2014).